Tetrahedron Vol. 49, No. 45, pp. 10239-10252, 1993
Printed in Great Britain

0040-4020/93 $6.00+.00

Studies on a Hydrocarbon Capped Free Base Tetraphenylporphyrin and its Conjugate Acids - First Observation of a Monoprotonated Tetraphenylporphyrin {CapTPP(H_3^+)$CF_3CO_2^-$}

Örn Almarsson, Andrei Blaskó and Thomas C. Bruice*

Department of Chemistry
University of California at Santa Barbara
Santa Barbara, CA 93106

(*Received in USA* 26 *July* 1993; *accepted* 8 *September* 1993)

ABSTRACT: ^{1}H-NMR and visible absorbtion spectroscopic titrations of a unique hydrocarbon capped porphyrin $3H_2$ with trifluoroacetic acid in chloroform result in the formation of a monoprotonated porphyrin species $3H_3^+\{CF_3CO_2^-\}$. This represents the first observation of a monobasic tetraphenylporphyrin acid. The monocation forms the dibasic $3H_4^{2+}\{CF_3CO_2^-\}_2$ upon further addition of acid. Back-titration of $3H_4^{2+}\{CF_3CO_2^-\}_2$ with DMSO demonstrates that the monocation can be generated from the diacid as well as the free base porphyrin. The capping structure on one face of the tetraphenylporphyrin is suggested to diminish the extent of solvation of one proton of $3H_4^{2+}\{CF_3CO_2^-\}_2$ by $CF_3CO_2^-$, thereby rendering the first dissociation constant (represented by $C_{50(1)}$) considerably larger than the second dissociation ($C_{50(2)}$). ^{19}F NMR chemical shifts of the counterions at -50°C show a similarity to the $CF_3CO_2^-$ counterions of $TPPH_4^{2+}\{CF_3CO_2^-\}_2$ and indicated a strong association with the porphyrin acid species. 2D NMR ROESY spectroscopy with Distance Geometry Refinement afforded a solution structure for $3H_2$, from which representative structures of possible inclusion compounds $3H_3^+\{CF_3CO_2^-\}$ and $3H_2\{CHCl_3\}$ were created by molecular modeling. Although the dome of the capping structure is predicted to be large enough to accommodate a trifluoroacetate anion on the inside, ^{19}F NMR spectra and FAB-mass spectra do not support the presence of an acid-base inclusion compound.

INTRODUCTION: The diacidic porphyrin bases protonate in the presence of strong acids, such as trifluoroacetic acid, to give the porphyrin dication $1H_4^{2+}$.[1] The free base porphyrin $1H_2$ has a brownish-red color, which upon protonation gives way to the deep emerald green color of the porphyrin dication $1H_4^{2+}$. Tautomerism in free-base porphyrins, as well as the nature of conjugate acids of porphyrin have been studied. Low temperature ^{1}H NMR was used as early as 1972 by Storm and Teklu[2] to slow the tautomeric shifts of pyrrolic N-H protons which occur in free base

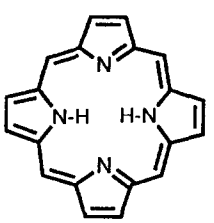

$1H_2$

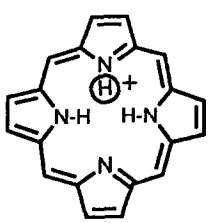

$1H_3^+$

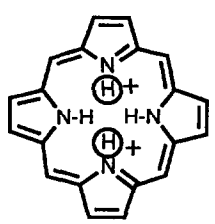

$1H_4^{2+}$

porphyrins. It was concluded that the most stable tautomer form has the structure of $1H_2$. More recently, Schlabach et al. used variable temperature NMR to elucidate pathways for tautomeric shifts in a variety of porphyrins.[3] Sanders and coworkers have used a cyclic trimer[4] of free base tetraphenylporphyrins as a selective ligand for large anions. The interactions of weak Brønsted bases with 5,10,15,20-*meso*-tetraphenylporphyrin ($2H_2$) dications $\{2H_4^{2+}(X^-)_2\}$ have been studied

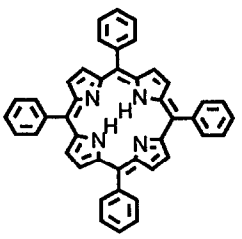

$2H_2$

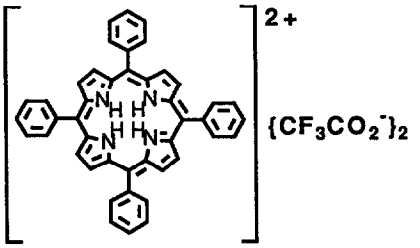

$[2H_4^{2+}]\{CF_3CO_2^-\}_2$

in our laboratory.[5] It was found that weak bases, such as dimethylformamide (DMF) and dimethylsulfoxide (DMSO), are able to deprotonate the dicationic species to regenerate the free base TPP without a detectable intermediate monoprotonated porphyrin. The monocationic $1H_3^+$ species have proven to be elusive. A crystal structure of octaethylporphyrin monocation $\{OEP\text{-}H_3^+\}\cdot I_3^-$ [6a] and a spectral study[6b] of the same compound are the only investigations into the properties of $1H_3^+$. While the X-ray structure does not resolve the positions of the protons in the molecule, tilting of one pyrrole ring in the porphyrin skeleton was postulated to arise from protonation of the ring. Steric crowding prevents the N-H bonds of $1H_3^+$ and $1H_4^{2+}$ from being in one plane. Particularly interesting is the complete lack of reports of $TPPH_3^+$ ($2H_3^+$) species, for which the present paper will provide a remedy.

We have engaged in the syntheses and structure elucidations of superstructured tetraphenylporphyrin (**TPP**, $2H_2$) derivatives as possible models for a variety of enzymatic systems which employ porphyrin cofactors.[7] One of these efforts resulted in the synthesis of a uniquely hydrocarbon capped TPP[7a], $C_{68}H_{70}N_4$ ($3H_2$, Chart I). This porphyrin has, among other interesting properties, eminent solubility in petroleum ether. The complete lack of heteroatoms and acid labile

Chart I

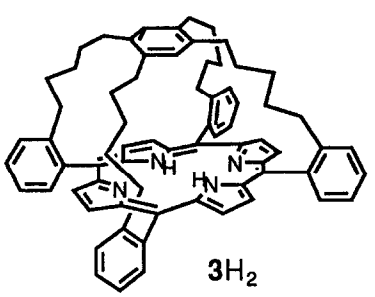

$3H_2$

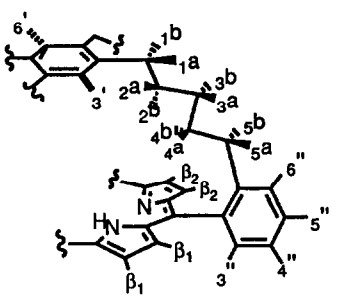

groups (esters, amides) in the capstructure makes this porphyrin suitable for study of chemistry under forcing conditions (e. g. strong acid or oxidant).[8] The present paper deals with structural studies on the free base hydrocarbon capped tetraphenylporphyrin $3H_2$ (Chart I) and its conjugate acids $3H_3^+$ and $3H_4^{2+}$ in chloroform, using NMR and visible spectroscopy. Two-dimensional NMR, coupled with Distance Geometry[9] refinement and molecular mechanics minimizations, was used to calculate a representative solution structure for the free base porphyrin. The structure for $3H_2$ was used to generate models for the possible inclusion compounds $[3H_3^+]CF_3CO_2^-$ and $[3H_2]\{CHCl_3\}$. Low temperature ^1H NMR, as well as ^{19}F NMR, of the intermediate $[3H_3^+]CF_3CO_2^-$ and $[3H_4^{2+}]\{CF_3CO_2^-\}_2$ allowed further characterization of the nature of the complexes. This represents the first reported observation of a stable tetraphenylporphyrin monoacid ($TPPH_3^+$) species.

RESULTS AND DISCUSSION. Synthesis and characterization of the hydrocarbon capped porphyrin $3H_2$, the compound of this study, has been reported previously.[7a] An improvement in the yield of porphyrin was achieved by direct BF_3-etherate catalyzed condensation of tetraacetal **4**[7a] with pyrrole to give $3H_2$ (Scheme I). The reaction

Scheme I

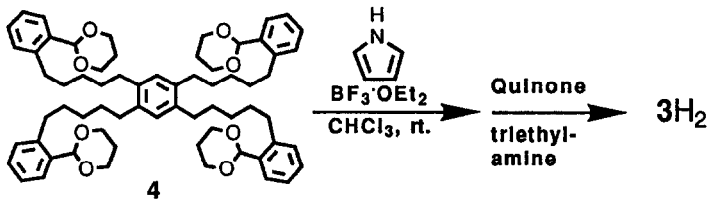

4

in chloroform could be run at significantly higher concentration than previously required. Thus, $2x10^{-3}M$ solution of tetra-(1,3-dioxane)acetal **4** in chloroform and $[BF_3{\cdot}Et_2O] = 5x10^{-4}M$ with stirring for 1 hour in the dark under argon, followed by DDQ oxidation used in the standard Lindsey method[10,11] afforded in the best instance 8% of $3H_2$. The yield is better than previously obtained, and the deprotection of the tetrakis(1,3-dioxane acetal) **4** to give the corresponding tetraaldehyde precursor is avoided. This step was previously found to be rather inefficient.[7a] In addition to $3H_2$, an increase in yield of another isolable porphyrin product was observed. The porphyrin, which elutes after the highly non-polar capped porphyrin, is still obtained in a small yield and is highly fluorescent even when compared with other free base porphyrins. Relatively concentrated solutions (~5mg/ml) of this compound appear cloudy under UV light. Proton NMR indicates two types of capping benzene ring C-H's (upfield shifted to 5.5 ppm), as well as slightly upfield shifted N-H resonances. The UV-visible spectra show a red shifted Soret band (λ_{max} = 414 nm, compared with λ_{max} = 418 nm for $3H_2$) with a characteristic shoulder indicating a free-base porphyrin. The mass spectrum (Fast atom bombardment, FAB) gave a molecular ion at approximately 3839 m/z. We tentatively propose the trimer structure **5** (shown in stereo view) for this compound. The stacking of the aromatic rings in **5** is consistent with upfield shifts of N-H resonances in ^1H NMR and red-shifting of the Soret in the electronic spectrum. The chain-like structure of **5** is anticipated, since

1,2,4,5-tetraalkyl benzene derivatives are expected to prefer the "up-down-up-down" alternating regiochemistry for the alkyl groups around the ring to other arrangements.[12]

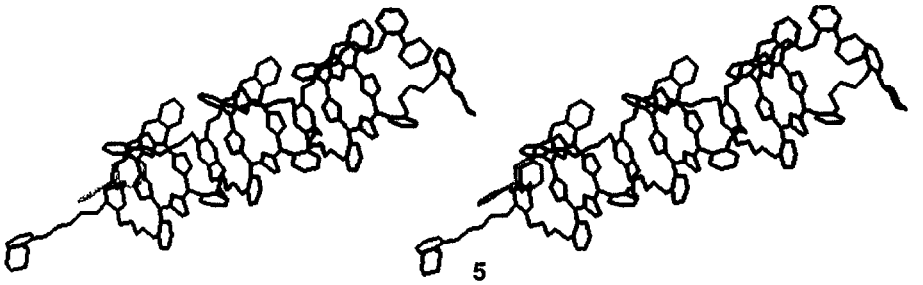

5

Characterization of the C5 capped porphyrin was achieved with the complete assignment of all proton resonances by two-dimensional NMR methods. The contour plot of Figure 1a shows the result of a DQF-COSY[13] experiment. The spectrum confirms previous assignments in the aromatic region[7a] but of particular importance here is the assignment of the five contiguous methylenes of the

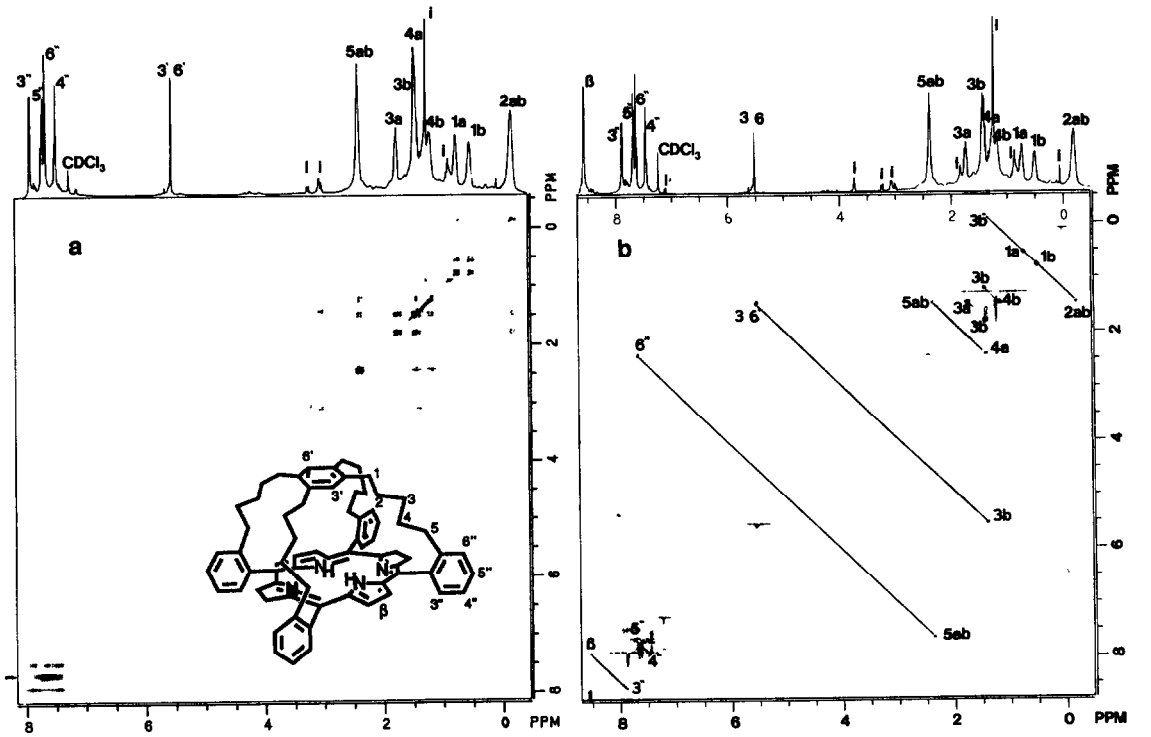

Figure 1: (a) DQF-COSY contour plot of $3H_2$ in $CDCl_3$ at 25°C.
(b) ROESY contour plot of $3H_2$ in $CDCl_3$ at 25°C with a mixing time of 200 ms.

chains linking the cap to the ortho-positions of TPP. These signals appear as broad singlets at room temperature in the region between 2.4 and -0.2 ppm. The only combination of assignments consistent with the observed cross-peak pattern in this region is the following (refer to Chart I for numbering of methylenes): The two broad peaks at 0.74 and 0.51 ppm give cross peaks with each other and with the resonance at -0.19 ppm. The signal at -0.19 ppm also gives cross peaks with the resonances at 1.74 and 1.44 ppm, which requires the resonance to be for a $-CH_2-$ in the middle of the chain. The resonances at 1.74 and 1.44 ppm give cross peaks with the resonances at 1.33 and 1.18 ppm and the latter ones J-couple with the signal at 2.39 ppm. The ROESY spectrum (Figure 1b) shows that the resonance at 2.39 ppm has proximities with the aromatic region of the *meso*-phenyl rings, i. e. with the 6" resonance. The signal at 2.39 ppm therefore belongs to 5ab (Table 1, Figure 1) and the resonances at 0.74 and 0.81 ppm were assigned to 1a and 1b, respectively. Chemical shifts and assignments are listed in Table 1.

Table 1. ^1H NMR Chemical Shift Assignments of $3H_2$ in $CDCl_3$ at 25°C.

Proton	δ(ppm)	Proton	δ(ppm)
2ab	-0.186	5ab	2.389
1b	0.513	3',6'	5.518
1a	0.743	4"	7.458 t (J = 6.5 Hz)
4b	1.183	6"	7.631 d (J = 7 Hz)
4a	1.375	5"	7.683 t (J = 6.5 Hz)
3b	1.436	3"	7.887 d (J = 6 Hz)
3a	1.740	β-pyrrole	8.567 (2 signals, Δδ~2Hz)

The downfield shift of 5ab and the upfield shift of 2ab are consistent with the ROESY-Distance Geometry derived 3D-structure (vide infra).

Solution structure for $3H_2$ in $CDCl_3$ by ROESY measurements and Distance Geometry refinement. While the DQF-COSY helps to further substantiate the structure of $3H_2$, the use of the **R**otating frame **O**verhauser **E**ffect **S**pectroscop**Y**[14] experiment provides NOE enhancements between proximal protons in the molecule. Quantification of the distances between protons involved in ROESY interactions is done by relating the NOE enhancements to internuclear separations (see experimental section). Application of the Distance-Geometry program[9] with NMR constraints and molecular mechanics minimization in $CHARM_m$[15] ultimately results in the generation of a representative solution structure(s) of the molecule. Figure 1b shows the ROESY spectrum for $3H_2$ in $CDCl_3$ at a mixing time of 200 ms. Proximities were seen between 5ab leg methylene protons and 6" ortho *meso*-phenyl protons (Chart I). This interaction confers a noninteractive position of 5ab with the porphyrin ring and their chemical shifts are consistent with a $-CH_2-$ attached to a phenyl ring (2.4 ppm) and thus they do not experience the anisotropic shielding associated with proximity to the top of the porphyrin plane. As expected, 5ab has ROESY peaks with 4a. The 3b methylene protons have proximities with 2ab $-CH_2-$ and 3',6' hydrogens of the

capping benzene ring. The 3b methylene protons are slightly overlapped with 4a -CH_2's. We assigned the ROESY peak of 3b with regard to the cap. Interaction was also noted between β-pyrrole protons and 3", 5" and 4" and between the geminal protons, strongly dominated by spin diffusion (Figure 1b). A total of 18 distance constraints were derived (see experimental and Table 2). Although the 5ab-4a and 3b-2ab distance constraints do not bear much structural information,

Table 2. ROESY and Molecular Mechanics Refined Interproton Distances (Å) in $3H_2$

H_i-H_j	Exp.[a]	Calc.[b]	H_i-H_j	Exp.[a]	Calc.[b]
β - 3"	2.97	3.15	3',6' - 3b	2.65	3.14
5" - 4"	2.46[c]	2.47	5ab - 4a	2.83	2.75
6" - 5ab	2.73	2.48	3b - 2ab	2.76	2.75

[a]from ROESY data, according to eq. 3 (experimental section)
[b]from minimized structure from DGEOM/$CHARM_m$ refinement Values are averages of all four interactions in the molecule
[c]standard for ROESY distances.

they were used along with the other constraints (β-3", 6"-5ab and 3'(6')-3b). The upper limits of the interactions were set at 15% higher than the distance evaluated by ROESY calculation, while the lower limit was set at the sums of van der Waals radii. The distance constraints were used in the Distance Geometry program along with a $CHARM_m$ mimimized structure of $3H_2$ to generate 100 structure which accommodate the constraints. The structures were grouped into conformational families based on RMS differences of their coordinates (see experimental) and finally $CHARM_m$ minimizations were performed to compare representatives from each family of conformers. The structure of lowest $CHARM_m$ potential energy is presented as a stereo pair in Figure 2. The structure shows some slipping of the benzene cap to one side of the porphyrin ring, creating a slight deviation from the C_{2v} symmetry observed by NMR at ambient temperature (vide infra).

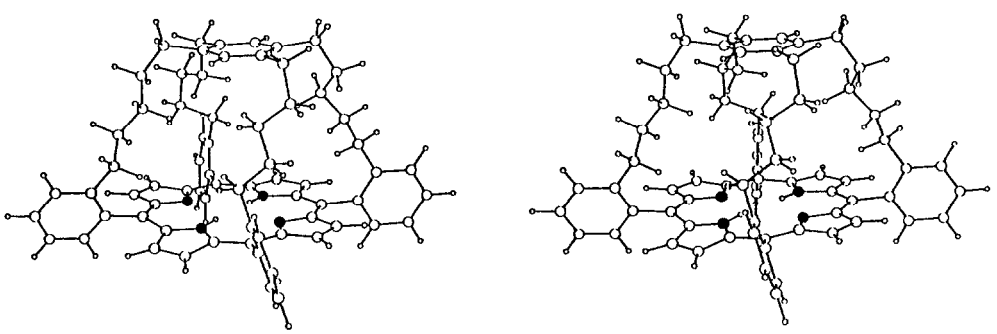

Figure 2 Stereo view of $3H_2$ in chloroform obtained by DGEOM/molecular mechanics refinement of the ROESY data in $CDCl_3$ at 25°C.

Variable temperature ^{1}H NMR spectra of $3H_2$ in $CDCl_3$ solution were obtained on a GN-500 spectrometer operating at 500 MHz. Cooling of the probe was conducted stepwise, with accumulation of spectra at 10 degree intervals. Overlays of proton spectra during the course of cooling from room temperature to -50°C are shown in Figure 3. At 25°C, the region of porphyrin β-

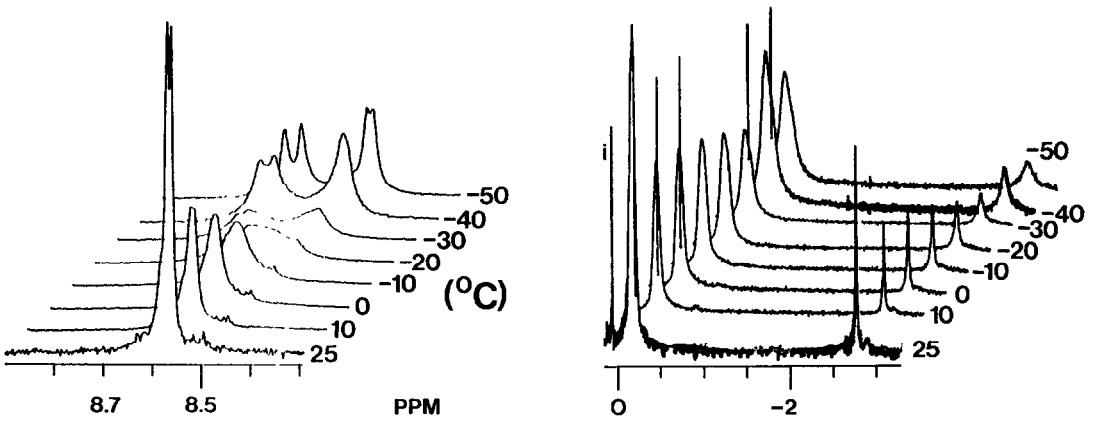

Figure 3. ^{1}H NMR spectra of $3H_2$ in the aromatic and pyrrolic N-H regions at the indicated temperatures.

pyrrole protons (downfield of 8 ppm vs. TMS) displayed two singlets, narrowly spaced ($\Delta\delta < 2$ Hz). At the final temperature of -55°C, four signals had separated in this region: The resonances appear as pairs of two signals at 8.5 and 8.7 ppm, the peak separation within each pair being 10 and 18 Hz, respectively. The peak separation cannot be ascribed to vicinal coupling, due to the size of the separations and their variation with temperature. Two explanations are possible for the four peaks: i) Exchange of the N-H protons on the pyrrole rings is slowed sufficiently such that a single tautomer is observed on the NMR time scale, or ii) slow shifting (lateral slipping) of the capping benzene ring on top of the porphyrin of $3H_2$ is occurring at low temperature, while at elevated temperature the cap slides from one side to the other to afford an average structure of C_{2v} symmetry (Scheme II).

Scheme II

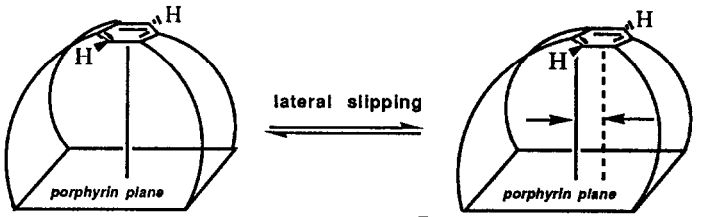

Average structure (ambient temperature) *"Frozen" structure (low temperature)*

The latter explanation seems more plausible, since the N-H resonances have not sharpened nor separated sufficiently at -50°C (Figure 3). A hump is detected on the high-field side of the N-H resonance at this temperature, which may indicate the ensuing separation of two peaks. As

suggested in Scheme II, the capping benzene protons are expected to slip across the porphyrin plane by the same distance, since the signal at 5.52 ppm broadens only slightly upon cooling. This indicates that the 3',6' protons are in very similar magnetic environments and thus their signals do not separate significantly at low temperature.

Titration of $3H_2$ in $CDCl_3$ solution with trifluoroacetic acid (TFA, 1M in $CDCl_3$) resulted in the formation of conjugate acids of the capped porphyrin. Figure 4 shows proton spectra at -50°C recorded during a representative titration experiment. When less than 1 equivalent of TFA has been added, the β-pyrrole signals undergo a substantial broadening and coalesce into a signal with a linewidth of 250 Hz. The sharp singlet of the capping benzene hydrogens at 5.52 ppm as well as the N-H resonance also broaden noticably. In the region upfield from TMS, the broad $-CH_2-$ resonance for methylene group 2 of the chain (see Chart I and Figure 4) at 0.1 ppm disappears and

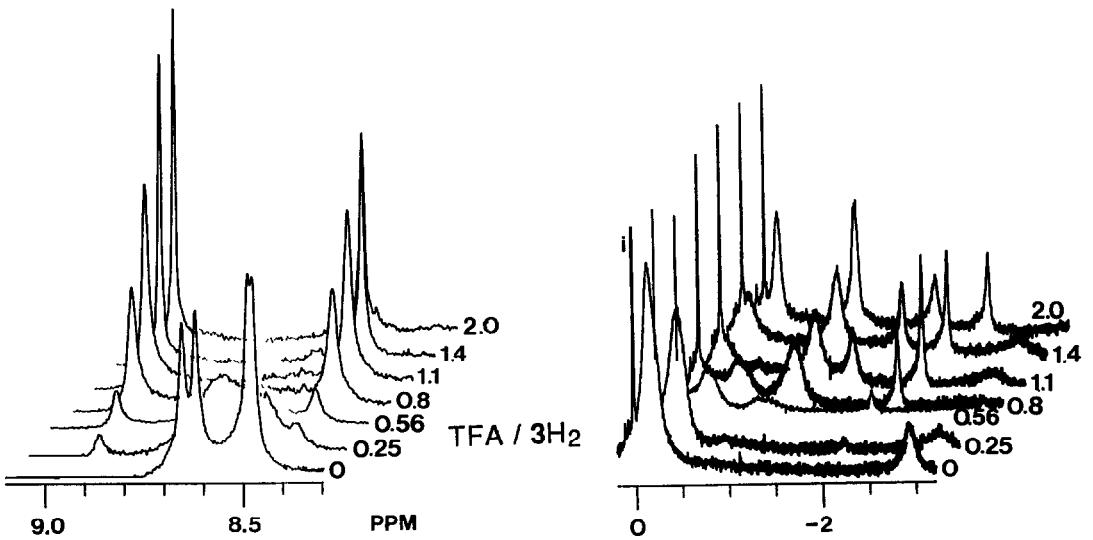

Figure 4: ^1H NMR spectral titration of $3H_2$ in $CDCl_3$ ($8x10^{-4}M$) with trifluoroacetic acid (TFA) at -50°C. The numbers beside each spectrum indicate the mol ratios of TFA to $3H_2$.

two new signals emerge, on both sides of the disappearing resonance. The low-field signal integrates to 8H, while the high-field signal integrates to 1H, and is exchangable by addition of DCl/D_2O. These observations speak for the presence of an unsymmetrical intermediate state, presumably the monocation $3H_3^+$. The presence of this intermediate is further supported by electronic spectral titration (vide infra). To the best of our knowledge, this is the first report of a TPP-H_3^+ species that is a stable intermediate state in solution.

Upon addition of 1-2 eq. of TFA, the NMR spectral features begin to sharpen in the β-pyrrole region, where two sharp and well separated singlets appear, indicating a C_{2v} symmetric species. The capping benzene ring protons again appear as a sharp singlet at 5.5 ppm, only slightly shifted with respect to the signal for the free base porphyrin. The N-H resonance appears further upfield

and is broader than previously. Even after 2 eq. of added TFA the signal only integrates to little more than 1H. Between the ratio 2:1 to 3:1 TFA/porphyrin (spectra not shown in Figure 4), there is no detectable change in the ^{1}H NMR spectrum at -50°C. The integral of the N-H resonance is still only 1.2 - 1.4 protons, which indicates that exchange is very rapid, at least for one of the protons in the porphyrin acid species. The compound present in the largest amount after 0.8 eq. TFA is presumably the symmetric porphyrin diacid, $3H_4^{2+}$. The characteristic visible spectrum, with a Soret band at 438 nm, confirms this conclusion. When the temperature is raised above -30°C, the high-field region of the N-H resonances diminishes and falls into the baseline. Back-titration of $3H_4^{2+}$ at -50°C to regenerate the free base was achieved using the weak Brønsted base DMSO-d6. Again, it was possible to observe the intermediate monocation $3H_3^+$ which had a spectrum virtually indistinguishable from the spectrum obtained when titrating with acid.

Visible absorbtion spectroscopic titration of $3H_4^{2+}\{CF_3COO^-\}_2$ with dimethylsulfoxide (DMSO) gives further evidence for the presence of the intermediate monocation. Titration of $3H_4^{2+}\{CF_3COO^-\}_2$ in $CHCl_3$ at 10^{-6} M with DMSO was performed by the method used in a previous study[5] and a typical spectral overlay is shown in Figure 5a. With added DMSO the dication absorbance at 438 nm diminishes to yield an intermediate at 422 nm, which finally goes to the free base at 418 nm. Two isosbestic points are observed (Figure 5a) and the monoprotonated species appears stable under the conditions. The same type of spectral overlays were obtained when the the free base was titrated with TFA. This observation of a stable $3H_3^+\{CF_3COO^-\}$ contrasts with similar experiments with TPP, where no intermediate could be observed by absorbtion spectroscopy.[5,16] From the data in Figure 5a it was possible to derive values for C_{50} for the processes of eq. 1 and 2:

$$3H_4^{2+}\{CF_3CO_2^-\}_2 + Me_2S{=}O \underset{}{\overset{C_{50(1)}}{\rightleftharpoons}} 3H_3^+\{CF_3CO_2^-\} + Me_2S{=}O\text{-}H^+\{CF_3CO_2^-\} \quad (1)$$

$$3H_3^+\{CF_3CO_2^-\} + Me_2S{=}O \underset{}{\overset{C_{50(2)}}{\rightleftharpoons}} 3H_2 + Me_2S{=}O\text{-}H^+\{CF_3CO_2^-\} \quad (2)$$

The plots of Figure 5b show the changes in absorbtion at 438 and 418 with added DMSO. The C_{50} values were obtained by locating the DMSO concentration where half of the cationic species ($3H_4^{2+}\{CF_3COO^-\}_2$ for $C_{50(1)}$ and $2H_3^+\{CF_3COO^-\}$ for $C_{50(2)}$) had reacted (Figure 5b). A C_{50} of 0.072 was previously calculated for the $TPPH_4^{2+}\{CF_3COO^-\}_2$ system reacting with DMSO in chloroform.[5] The value for $C_{50(1)}$ of 0.026 for $3H_4^{2+}\{CF_3COO^-\}_2$ is small compared with C_{50} for $TPPH_4^{2+}\{CF_3COO^-\}_2$ and indicates that the former is more readily deprotonated by DMSO. The value for $C_{50(2)}$ for $3H_3^+\{CF_3COO^-\}$ was calculated from the increase in absorbance at 418 nm as shown in Figure 5b. Comparison of the values of 0.048 for $C_{50(2)}$ and 0.026 for $C_{50(1)}$ explain why it is possible in this case to observe the monocationic intermediate: The special combination of counterion, solvent and titrant Brønsted base brings the values for C_{50} for the mono- and dicationic species of **3** into comparison. The absence of detectable intermediate monocation in previous experiments was due to the rapid deprotonation of $TPPH_3^+$. Stabilization of the intermediate

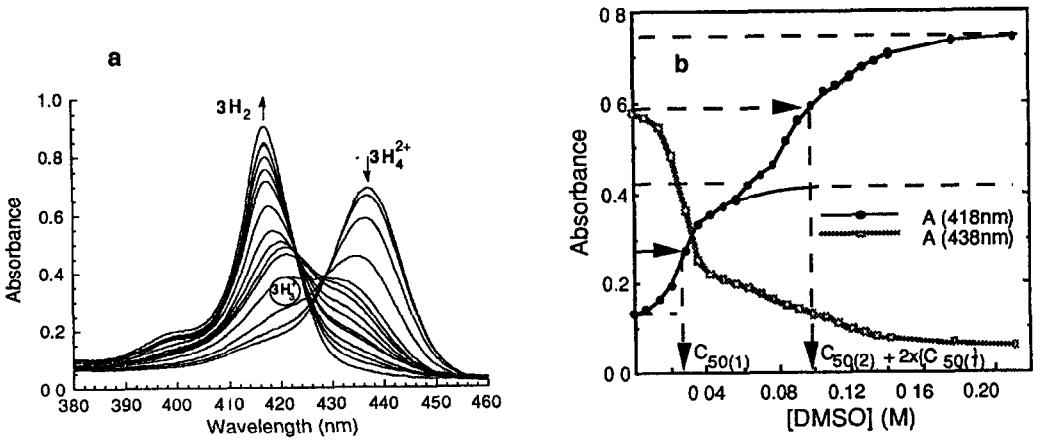

Figure 5 (a) Visible absorbtion spectroscopic titration of $3H_4^{2+}\{CF_3COO^-\}_2$ ($1x10^{-6}$M) with DMSO in chloroform at 25°C. (b) Plots of absorbances at 418 nm and 438 nm vs. total concentration of DMSO in a titration of $3H_4^{2+}\{CF_3COO^-\}_2$

$3H_3^+\{CF_3COO^-\}$ relative to the dication is undoubtedly due to the presence of the capstructure in the unique hydrocarbon capped porphyrin **3**.

Modeling of the structures for $[3H_3^+]CF_3CO_2^-$ and $[3H_2]\{CHCl_3\}$ is of interest, since the the presence of the cap introduces the possibility for the counterion(s) or chloroform solvent (Figure 6a and b) residing inside or outside the capstructure. The structure for $3H_2$ from 2D NMR-DGEOM refinement (Figure 2) was used to build structures for possible inclusion compounds of $3H_2$. Placement of one $CF_3CO_2^-$ was performed inside the cap unit A molecule of chloroform was also

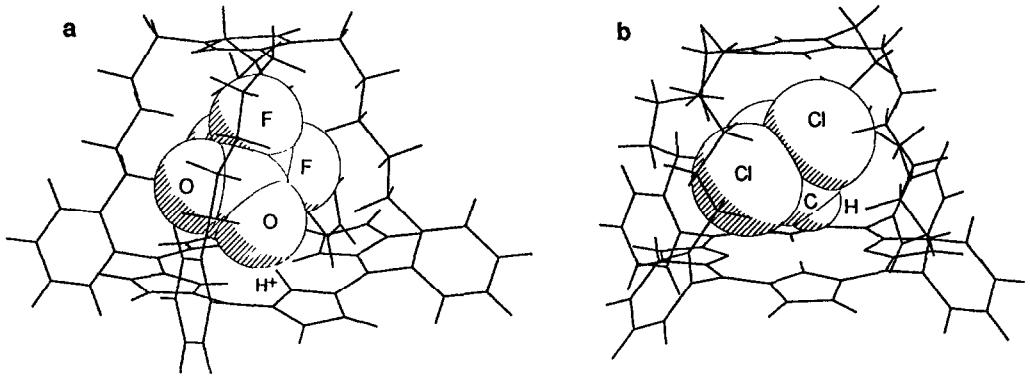

Figure 6 (a) Minimized structure of $3H_2\{CF_3CO_2^-\}$, where the anion is present inside the cap. (b) Structure of $3H_2\{CHCl_3\}$ inclusion compound, modeled using the ROESY structure of $3H_2$

placed inside the capstructure of $3H_2$. Figures 6a and b show the structures of $[3H_3^+]CF_3CO_2^-$ and $[3H_2]\{CHCl_3\}$ inclusion compounds, respectively. In the case where $CF_3CO_2^-$ was placed inside the cap, minimization of the entire structure was necessary to accommodate the anion. In contrast, $CHCl_3$ fitted into the cap without necessary adjustments to the porphyrin cap skeleton. Therefore, the chloroform molecule was allowed to adjust within the cavity created by the rigid cap of $3H_2$ structure, calculated from ROESY data (Figure 2). For comparison with the structure in Figure 6a, a trifluoroacetate anion was placed outside the cap on the open face of the porphyrin ring of $3H_2$, within hydrogen bonding distance of the pyrrole nitrogens. Energies from the $CHARM_m$ forcefield employed indicated that the anion of the monobasic $[3H_3^+]CF_3CO_2^-$ prefers sitting inside the dome of the porphyrin to maximize van der Waals attractions (Figure 6a). This arises from the complete lack of solvation in our model. As seen in Figure 6b, it is possible for the chloroform molecule to reside inside the cap, but acid-base hydrogen bond interaction present in the hypothetical inclusion compound of Figure 6a are absent. The $CHCl_3$ molecule is capable of acheiving stabilizing van der Waals interactions in the interior and moreover appears able to traverse the openings to the exterior with greater ease than $CF_3CO_2^-$.

Fluorine-19 NMR investigations of conjugate acids of $3H_2$ in $CDCl_3$ were performed to probe the possibility of an inclusion compound, as suggested in Figure 6a. First, $3H_2$ was titrated at -50°C with CF_3COOH with observation of ^{19}F resonances and relating them to CF_3COOH (external standard in a coaxial inset tube). The stack plot of Figure 7 indicates slight shifting of the fluorine signal at -1.5 ppm vs. CF_3COOH as the titration proceeds. Broadening is

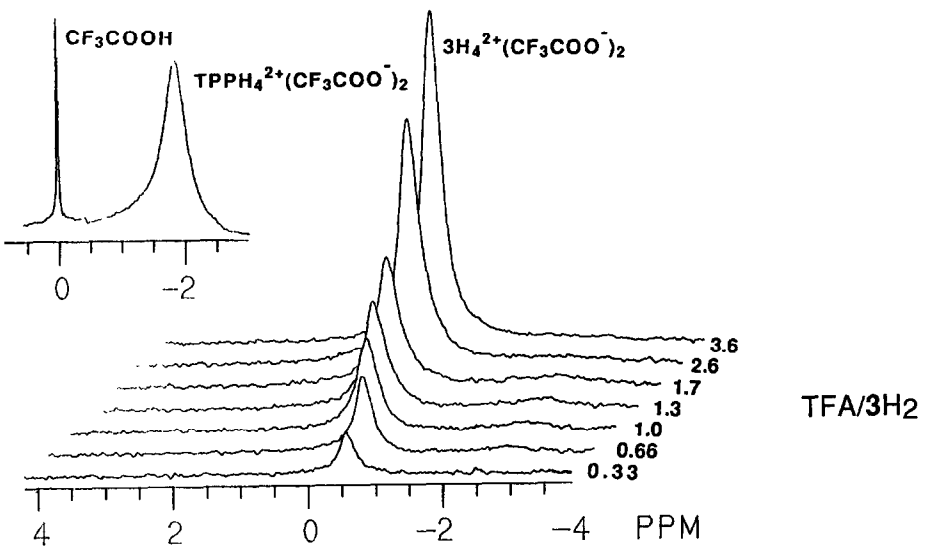

Figure 7 ^{19}F NMR titration of $3H_2$ in $CDCl_3$ with TFA at -50°C. The mol ratios of TFA/$3H_2$ are indicated beside each spectrum. Inset ^{19}F spectrum of $TPPH_4^{2+}[CF_3CO_2^-]_2$ at -50°C, including the signal of the internal reference, CF_3COOH in $CDCl_3$)

observed but no splitting into two signals is seen. The position of the signals indicates tight ion pairs, resulting in a small upfield shift relative to CF_3COOH. For comparison, $\mathbf{TPPH_4}^{2+}[CF_3CO_2^-]_2$ was produced by addition of trifluoroacetic acid to a solution of TPP in $CDCl_3$. The ^{19}F spectrum of the adduct is shown in the inset to Figure 7. The signal at -1.0 ppm is significantly broader than that for $\mathbf{3H_2}$. adducts with CF_3CO_2H. Comparison of the spectra suggest that the association of $CF_3CO_2^-$ counterion is similar in both cases and that the capstructure does not prevent the counterion association. Greater upfield shifts would be expected for a fluorine atom inside an aromatic host.[17]

Mass spectral analyses of $[\mathbf{3H_4}^{2+}]\{CF_3CO_2^-\}_2$ and $[\mathbf{TPPH_4}^{2+}]\{CF_3CO_2^-\}_2$ were carried out to further investigate the possibility of an inclusion compound or **3** and $CF_3CO_2^-$ when the porphyrin is protonated. Mass spectroscopy was performed by the **F**ast **A**tom **B**ombardment (FAB) method, using nitrobenzyl alcohol as the matrix. The samples were prepared in $CHCl_3$ and evaporated to dryness. The FAB results indicate in both cases the generation of free porphyrin cations $[\mathbf{3H_3}^+]$ and $[\mathbf{TPPH_3}^+]$ with no evidence for preferential retention of one $CF_3CO_2^-$ entity inside the cap of $[\mathbf{3H_3}^+]$. The combined results of ^{19}F NMR and mass spectroscopy rule out the existence of an acid-base inclusion compound of $\mathbf{3H_2}$ with trifluoroacetic acid.

CONCLUSION: The study reports the first observation of a $\mathbf{TPPH_3}^+$ species, observable at room temperature in dilute $CHCl_3$ solutions with visible absorbtion spectroscopy, and at low temperatures by proton NMR. The observation of the monocationic intermediate is made possible by the presence of the stable capstructure on one face of porphyrin **3**, which hinders access of one counterion to the porphyrin diacid and stabilizes $\mathbf{3H_3}^+$ relative to $\mathbf{3H_4}^{2+}$ by decreasing the solvation of a proton on the pyrrole nitrogen. ROESY experiments coupled with Distance Geometry refinement and molecular mechanics minimizations afforded a representative solution structure for $\mathbf{3H_2}$ in $CHCl_3$. Although structures obtained by molecular modeling indicate the possibility of an inclusion compound of trifluoroacetate and $\mathbf{3H_3}^+$, ^{19}F NMR and FAB mass spectra do not support the existence of such a complex. The possibility of a chloroform adduct still exists, but is much more difficult to test.

EXPERIMENTAL: The synthesis of $\mathbf{3H_2}$ was performed essentially as described previously[7a] with the exception that the tetraacetal **4** was used instead of a deprotected tetraaldehyde. After purification the samples obtained had spectral features identical with authentic samples of $\mathbf{3H_2}$ from our previous study. Absorbtion spectra were recorded on a Cary 14 UV-vis spectrophotometer interfaced with a Zenith computer employing OLIS (On-Line Intruments Systems Inc.) data acquisition and processing software. ^1H- and ^{19}F NMR spectra were obtained on a GN-500 spectrometer at 500.0 and 470.0 MHz, respectively. $CDCl_3$ stored over anhydrous potassium carbonate was employed as solvent (Aldrich 99.99% atom D). ^1H-chemical shifts (ppm) were referenced to tetramethylsilane. 5,10,15,20-*meso*-Tetraphenylporphyrin (TPP-H_2) was purchased from Alfa Products Co. and used without purification. Trifluoroacetic acid (TFA) was obtained from Fluka and used as received. ^{19}F chemical shifts were referenced to TFA, placed in a coaxial inset tube at $1x10^{-3}$ M in $CDCl_3$. The standard was used initially to calibrate the signal positions, but was

removed so as not to interfere with the signal due to anions associated with $3H_2$. DMSO-d6 was purchased from Aldrich (99.99% D atom). Chloroform and DMSO were obtained from Fisher and distilled prior to visible titrations. Chloroform was refluxed over potassium carbonate and distilled under argon. DMSO was distilled from calcium hydride under argon. NMR titrations were performed by adding trifluoroacetic acid in aliquots to solutions of $TPPH_2$ in $CDCl_3$ (10^{-3} M) at -50°C until the porphyrin dications were produced. Back-titrations with DMSO-d_6 were then performed. Addition of titrants was performed under argon with Hamilton microsyringes to 5 mm NMR tubes capped with a septum.

ROESY spectra were collected using the Kessler pulse sequence:[14] $90°_x$-t_1-$(\beta_y$-$\tau)_n$-aquisition. Spectra were collected into 4K data blocks for 512 t_1 increments with a relaxation delay of 3 s, β_y=4 μs, τ=18 μs, n=9091 to give a mixing time of 200 ms with a locking field strength of 3 kHz and spectral width in both dimensions of 6578.94 Hz. Data matrix was zero filled to 2 K and apodized with gaussian function to give a line broadening in both dimensions of 4 Hz. Quantitative data were obtained using eq. 3, which includes also the offset correction, where r_{ab} is the distance

$$r^6_{ab} = K \cdot \sin^2(\beta_a) \cdot \sin^2(\beta_b) / I_{ab}$$
$$\beta_i = \text{arctg}(\gamma B_{SL}/\omega_i) \qquad (3)$$

between protons a and b, B_{SL} the field strength of the locking field, γ the magnetogyric ratio, ω_i the resonance offset of nucleus i and K a constant evaluated from the cross peaks volume integral I_{ij} of proton i and j with known separation. Initial coordinates for $3H_2$ to be used with Distance Geometry[9] were generated as described in ref. 7a, footnote 5. The 18 distance constraints used with DGEOM were: 4 for β-3", 4 for 6"-5ab, 2 for 3'(6')-3b, 4 for 5ab-4a and 4 for 3b-2ab. Molecular modeling was performed on a Silicon Graphics 4D/320GTX workstation using the programs Quanta[18] (visualization and manipulation of structures) and $CHARM_m$[15] v 21.3 (energy minimizations). For $CHARM_m$ calculations, non-bonded interactions were cut-off at 14 Å and hydrogen bonds were considered within 4 Å and at angles between 90 and 270°. The adopted-basis Newton-Raphson (ABNR) algorithm was used for minimizations.

ACKNOWLEDGMENT: This work was supported by a grant from the National Institute of Health.

REFERENCES:

1 "Porphyrins and Metalloporphyrins" K. M. Smith (ed.), pp. 457-459, Elsevier, Amsterdam 1975.
2 Storm, C. C.; Teklu, Y. *J. Am. Chem. Soc.* **1972**, 94, 1745.
3 Schlabach, M.; Limbach, H.-H.; Bunnenberg, E.; Shu, A. Y. L.; Tolf, B.-R.; Djerassi, C. *J. Am. Chem. Soc.* **1993**, 115, 4554.
4 Anderson, H. A.; Sanders, J. K. M.; *J. Chem. Soc., Chem. Commun.* **1992**, 946.
5 Karaman, R.; Bruice, T. C. *Inorg. Chem.* **1992**, 31, 2454.

6 (a) Hirayama, N.; Takenaka, A.; Sasada, Y.; Watanabe, E.; Ogoshi, H.; Yoshida, Z. *J. Chem. Soc., Chem. Commun.* **1974**, 330. (b) Ogoshi, H.; Watanabe, E.; Yoshida, Z. *Tetrahedron*, **1973**, 29, 3241.

7 (a) Schnatter, W. F. K.; Almarsson, Ö.; Bruice, T. C. *Tetrahedron*, **1991**, 47, 8687. (b) Zhang, H. Y.; Blaskó, A. B.; Yu, J. Q.; Bruice, T. C. *J. Am. Chem. Soc.* **1992**, 114, 6621. (c) Bookser, B. C.; Bruice, T. C. *J. Am. Chem. Soc.*, **1991**, 113, 4208. (d) Karaman, R.; Bruice, T. C. *J. Org. Chem.* **1991**, 56, 3470. (e) Karaman, R.; Blaskó, A.; Almarsson, Ö; Arasasingham, R. D.; Bruice, T. C. *J. Am. Chem. Soc.*, **1992**, 114, 4889. (f) Karaman, R.; Jeon, S.; Almarsson, Ö.; Bruice, T. C. *J. Am. Chem. Soc.*, **1992**, 114, 4899. (g) Karaman, R.; Almarsson, Ö; Blaskó, A.; Bruice, T. C. *J. Org. Chem.* **1992**, 57, 2169. (h) Jeon, S. J.; Almarsson, Ö.; Blaskó, A. B.; Karaman, R. K. *Inorg. Chem.* **1993**, 32, 2562.

8 Fully hydrocarbon doubly strapped porphyrins have been synthesized: Tang, H.; Wijesekera, T. P.; Dolphin, D. *Can. J. Chem.* **1992**, 70, 1366. For other examples of capped porphyrins, see: (a) Baldwin, J. E.; Crossley, M. J.; Debernardis, J. F.; Dyer, R. L.; Huff, J. R.; Peters, M. K. *Tetrahedron* **1981**, 37, 3589. (b) Lindsey, J. S.; Mauzerall, D. C. *J. Am. Chem. Soc.* **1982**, 104, 4498. (c) Johnson, M. R.; Seok, W. K.; Ibers, J. A. *J. Am. Chem. Soc.* **1991**, 113, 3998.

9 (a) Crippen, G. M. in "Distance Geometry and Conformational Calculations", Bawden, D., Ed.; Research Studies Press, John Wiley, New York, **1981**. (b) Havel, T. F.; Kunoto, I. D.; Crippen, G. M. *Bull. Math. Biol.* **1983**, 45, 665. Examples of the successful use of Distance Geometry with NMR constraints to superstructured porphyrins are found in ref. 7b and 7h.

10 Lindsey, J. S; Wagner; R. W. *J. Org. Chem.* **1989**, 54, 828.

11 Previously, Zhang et al. (ref. 7b) showed that synthesis of a capped porphyrin from a tetraacetal precursor was more efficient that synthesis from the corresponding tetraaldehyde.

12 Conformational studies on highly substituted benzene rings have been performed with arene chromium complexes to elucidate stereodynamics of the alkyl substituents. See: Kilway, K. V.; Siegel, J. S. *J. Am. Chem. Soc.* **1992**, 114, 255 and references therein.

13 Martin, G. E.; Zekter, A. S. *Two Dimensional NMR Methods for Establishing Molecular Connectivity*; VCH Publishers: New York, 1988.

14 Kessler, H.; Griesinger, C.; Kerssebaum, R.; Wagner, E.; Ernst, R. *J. Am. Chem. Soc.* **1987**, *109*, 607.

15 Brooks, B. R.; Bruccoleri, R. E.; Olafson, B. D.; States, D. J.; Swaminathan, S.; Karplus, M. *J. Comput. Chem.* **1983**, *4*, 187.

16 Abraham, R. J.; Hawkes, G. E.; Smith, K. M. *Tetrahedron Lett.* **1974**, 71.

17 ^{19}F shifts are very sensitive to environment, and fall in a large range of values (several hundred ppm). See: Bovey, F. A. *Nuclear Magnetic Resonance Spectroscopy*; 2nd ed., Chapter 9, Academic Press: San Diego, 1988.

18 Quanta, version 3.2 from Molecular Simulations Inc., Waltham, MA, **1991**.